Nanoscale Metal Oxide Particles/Clusters as Chemical Reagents. Unique Surface Chemistry on Magnesium Oxide As Shown by Enhanced Adsorption of Acid Gases (Sulfur Dioxide and Carbon Dioxide) and Pressure Dependence

Jane V. Stark, Dong G. Park, Isabelle Lagadic, and Kenneth J. Klabunde*

Department of Chemistry, Kansas State University, Manhattan, Kansas 66056

Received December 5, 1995. Revised Manuscript Received March 14, 1996[⊗]

Surface adsorptive properties of nanoscale MgO particles have been compared with more conventional samples. Morphologically the nanoparticles (autoclave prepared = AP-MgO) are unique and very different from the conventional samples (conventionally prepared = CP-MgO), and AP-MgO possesses more defects, edge and corner sites, higher surface area and more higher index surfaces. The number of residual surface −OH groups/nm^2 is similar for both types of samples. Differences in adsorptivity of SO_2 and CO_2 at relatively low pressure (20 Torr) were determined by gravimetric means. Much larger quantities were adsorbed by AP-MgO. This process of chemisorption was dynamic, and oxygen scrambling occurred when SO_2 and $Mg^{18}O$ nanoparticles were in contact. These results, complying with FTIR studies, are rationalized as due to higher intrinsic surface reactivity coupled with higher concentrations of lower coordination ions on the nanoparticle. Pressure studies showed, however, that as 100 Torr of SO_2 or CO_2 was reached, the CP-MgO samples exhibited higher adsorptive capacities. Quantitative determinations of SO_2(CO_2) loading indicate that this difference can be attributed to multilayered physisorption on CP-MgO, which with its flatter, extended planes, can apparently form more ordered multilayered structures and thus physically adsorb more SO_2 (or CO_2). In the case of SO_3, large amounts of surface sulfates were detected by FTIR. Overall, our results indicate that nanoparticles of MgO possess a unique surface chemistry and their high surface reactivity coupled with a high surface area allowed them to approach the goal of being stoichiometric chemical reagents.

Introduction

The materials chemist finds magnesium oxide as a chemical of choice for theoretical and experimental studies of surface chemistry on ionic solids. This material is highly ionic with effective ionic charges close to ±2, whereas the MgO molecule is much more covalent with effective charges close to ±1.[1,2] Magnesium and oxygen coordinations of 4 and 5 result in polarization, but no significant electron density redistribution, leaving coordinations of 2 and 3 as having effective charges somewhere between ±1 and ±2. Totally ionic surfaces should limit chemisorption reactions to those involving electrostatic interaction and Pauli repulsion, while covalent contribution opens possibilities of direct covalent bonding and charge transfer, thus allowing more reaction possibilities at the surface of MgO.

Ab initio calculations with hydrogen are often used to probe perfect crystal surfaces and various surface defects.[3−6] Theoretical calculations have shown that the H_2 molecule has a small adsorption energy and does not dissociate on the perfect (100)MgO surface.[7] However, experimental studies using the temperature-programmed desorption method have shown that highly dispersed polycrystalline surfaces of MgO have a variety of active sites for hydrogen adsorption involving O−Mg pairs of low coordination, probably O_{3c}−Mg_{3c}.[4] In an IR study of magnesium hydrides, Coluccia and co-workers have also concluded that active chemisorption sites are cation−anion couples in low coordination on the surface.[5] Likewise, Knözinger and co-workers studied hydrogen adsorption on dispersed MgO and found heterolytic and homolytic dissociation, with the Mg_{3c}−O_{3c} site being dominantly responsible for the heterolytic dissociation.[8] More recently, theoretical studies showed that chemisorption energy depends strongly on coordination number and decreases in the following order: the valley site > Mg_{3c}−O_{3c} > Mg_{4c}−O_{3c}, with the latter two being only marginally bound if at all.[9] The valley site is in troughlike multicentered valleys on the microfaceted (111) surface. Studies by Onishi and co-workers of annealed MgO (111) surfaces and catalytic oxidative coupling studies have shown that this faceted (111) surface shows higher adsorption activity than the flat

[⊗] Abstract published in *Advance ACS Abstracts,* July 15, 1996.

(1) LaFemina, J. P. *Crit. Rev. Surf. Chem.* **1994**, *3*, 297.
(2) Abarenkov, I. V.; Antonova, I. M. *Phys. Status Solid B* **1979**, *93*, 315.
(3) Bauschlicher, C. W., Jr.; Lengsfield, B. H., III; Liu, B. *J. Chem Phys.* **1982**, *77*, 4084.
(4) Ito, T.; Kuramoto, M.; Yoshioka, M.; Tokuda, T. *J. Phys. Chem.* **1983**, *87*, 4411.
(5) Coluccia, S.; Boccuzzi, F.; Ghiotti, G.; Morterra, C. *J. Chem. Soc., Faraday Trans. 1* **1982**, *78*, 2111.
(6) Onishi, H.; Egawak, C.; Aruga, T.; Iwasawa, Y. *Surf. Sci.* **1987**, *191*, 479.
(7) Karimi, M.; Vidali, G. *Phys. Rev.* **1989**, *B39*, 3854.
(8) Knözinger, E.; Jacob, K. H.; Hofmann, P. *J. Chem. Soc., Faraday Trans. 1* **1993**, *89*, 1101.
(9) Sawabe, K.; Koga, N.; Morokuma, K.; Iwasawa, Y. *J. Chem. Phys.* **1994**, *101*, 6, 4819.

S0897-4756(95)00583-7 CCC: $12.00 © 1996 American Chemical Society

(100) surface, suggesting activity to be due to its valley sites and coordinatively unsaturated edge sites.[6,10]

Surface defects are as important, if not more important, for increased activity and are categorized as either extended defects, such as steps, kinks, and grain boundaries, or point defects, such as ion vacancies and substitutions.[11] It is known that the (001) surface of MgO rumples, with the surface cations moving inward and the surface anions moving outward from the surface. This movement of ions can result in Frenkel or Schottky type defects, as well as displaced ions on the surface. Reactions with H_2 arise from interaction with anion vacancies such as the self-trapped hole (O^- ion on the surface), the V^- center (one hole trapped near a cation vacancy), and the V center (two holes trapped near a cation vacancy).[12] Theoretical calculations of the electronic structure of neutral and charged surface oxygen vacancy defects (F_s, F_s^+, and F_s^{2+} centers) have found formation energies that agree with energy-dependent electron-energy-loss experiments.[13] It is believed by Lunsford and co-workers that these oxygen vacant holes or oxygen anionic vacancies with a trapped electron and a surface O^- species are responsible for the excellent catalytic activity of the Li/MgO oxidative coupling catalyst.[14] In addition to the surface O^- species mentioned, formation of superoxide ions, O_2^- have been discovered on (100) planes of MgO by electron paramagnetic resonance (EPR) investigation.[15] Oxygen species at the surface of metal oxides are important for their role in heterogeneous catalysis, corrosion, and contamination, but the superoxide ion is more special in that it can act as an electrophilic agent in catalytic oxidation processes.

Clearly, reactivity of MgO depends on the crystal faces exposed, surface ion coordination, electronic structure, and surface defects. It has also been shown that highly divided, high surface area, nanoscale particles of MgO are more active to decomposition of organophosphorus compounds[16−18] and have different intrinsic characteristics than their bulk counterparts.[19] The choice of precursor and method of preparation largely affect the activity of the MgO produced.[20,21] A review of the various preparation methods for highly divided MgO by Utamapanya[22] includes the methods of high-energy irradiation, thermal activation, and aerogel synthesis. Thus, it is proposed that by optimizing a particular preparation, MgO can be produced with specific characteristics to capitalize on for a desired reaction.

This study specifically will look at the intrinsic differences between bulk MgO (conventionally prepared = CP-MgO) and nanoscale MgO (autoclave prepared = AP-MgO) in relationship to morphology, reactivity, and, finally, active sites. Sulfur dioxide was used as an adsorbate due to its variety of possible bonding geometries and, for more practical reasons, for its environmental involvement in producing acid rain. It is produced in large amounts during coal combustion processes and is presently removed using calcium- and magnesium-based adsorbents forming sulfites and sulfates as final products. Using a more reactive form of MgO would benefit industry by reducing the amount of solid waste disposed, thus reducing the cost of disposal. Interest in gas−solid adsorption of SO_2 is also important for development of gas sensors and active catalysts, since SO_2 often poisons active sites on catalysts. Therefore, the nature of SO_2 interaction with MgO surfaces invites comprehensive investigation.

Overall, it is shown that nanoscale MgO particles adsorb much more SO_2 and CO_2 at low pressures, and this is due to enhanced surface reactivity and unique morphological features.

Experimental Section

(A) Preparation of Samples. The preparation of AP-MgO has been discussed earlier.[23] The reactions involved in this process are below.

$$Mg(s) + 2CH_3OH \rightarrow Mg(OCH_3)_2 + H_2(g)$$

$$Mg(OCH_3)_2 + 2H_2O \xrightarrow{\text{toluene}} Mg(OH)_2(gel) + 2CH_3OH(l)$$

$$Mg(OH)_2(gel) \xrightarrow{\text{hypercritical drying in autoclave}} Mg(OH)_2(aerogel)$$

$$Mg(OH)_2(aerogel) \xrightarrow{\text{heat treatment under vacuum}} MgO(s) + H_2O(g)$$

CP-MgO was prepared by hydrating 99.99% ultrapure magnesium oxide from Comprehenensive Research Chemical Corp. with excess distilled deionized water, heating it in air forming magnesium hydroxide and treating it under dynamic vacuum at the same conditions as AP-MgO.[24]

(B) Characterization of AP-MgO and CP-MgO. *(1) Desorbed Gases during Heat Treatment.* Since AP-MgO was produced from methoxide solution in toluene solvent, some residual carbon species were found remaining on the surface after heat treatment. To better understand the bonding nature of the surface species, AP-$Mg(OH)_2$ was heated under dynamic vacuum and portions of the gaseous products were removed using a liquid nitrogen cooled trap. The gas samples were trapped at reaction vessel temperature ranges of 100−120, 120−200, 200−300, 300−400, and 400−500 °C and analyzed by gas chromatography−mass spectrometry using 0.5 μL injections. A Perkin-Elmer QMass 910 was used with a HP1 cross-linked methylsilicone gum capillary column of 12 m × 0.2 mm × 0.33 μm film thickness, 99.99% ultrahigh-purity He carrier gas at ca. 20 mL/min, and column temperature and injector temperatures of 250 and 200 °C, respectively.

(10) Hargreaves, J. S.; Hutchings, G. J.; Joyner, R. W.; Kiely, C. J. *J. Catal.* **1992**, *135*, 576.
(11) Henrich, V. E. *Rep. Prog. Phys.* **1985**, *48*, 1481.
(12) Pope, S. A.; Guest, M. F.; Hillier, I. H.; Colbourn, E. A.; Mackrodt, W. C.; Kendrick, *J. Phys. Rev.* **1983**, *B28*, 2191.
(13) Gibson, A.; Haydock, R.; LaFemina, J. P. *Appl. Surf. Sci.* **1993**, *72*, 285.
(14) Shi, C.; Xu, M.; Rosynek, M. P.; Lunsford, J. H. *J. Phys. Chem.* **1993**, *97*, 216.
(15) Giamello, E.; Murphy, D.; Garrone, E.; Zecchina, A. *Spectrochim. Acta* **1993**, *49A*, 9, 1323.
(16) Li, Y. X.; Klabunde, K. J. *J. Chem. Mater.* **1992**, *4*, 611.
(17) Li, Y. X.; Koper, O.; Maher, A.; Klabunde, K. J. *J. Chem. Mater.* **1992**, *4*, 323.
(18) (a) Ekerdt, J.; Klabunde, K. J.; Shapley, J. R.; White, J. M.; Yates, J. T. *J. Phys. Chem.* **1988**, *92*, 6182. (b) Maher, A.; Klabunde, K. J. *Chem. Mater.* **1991**, *3*, 182. (c) Li, Y. X.; Klabunde, K. J. *Langmuir* **1991**, *7*, 1394.
(19) Itoh, H.; Utamapanya, S.; Stark, J. V.; Klabunde, K. J.; Schulp, J. R. *Chem. Mater.* **1993**, *5*, 71.
(20) Knözinger, I.; Jacob, K. H.; Singh, S.; Hofmann, P. *Surf Sci.* **1993**, *290*, 388.
(21) Choudhary, V. R.; Rane, V. H.; Gadre, R. V. *J. Catal.* **1994**, *145*, 300.
(22) Utampanya, S. Ph.D. Thesis, Department of Chemistry, Kansas State University, Manhattan, Kansas, 1990.
(23) Utamapanya, S.; Klabunde, K. J.; Schlup, J. R. *Chem. Mater.* **1991**, *3*, 175.
(24) Morris, R. M.; Klabunde, K. J. *Inorg. Chem.* **1983**, *22*, 682.

Quantitative measurements of the weight losses during heating were also conducted using 1.5 g samples of AP-MgO and CP-MgO heated under dynamic vacuum on a precalibrated quartz spring balance (for acid gas or chlorocarbon adsorption measurements).[25]

The attached calibrated magnifier allowed for precise measurements of the change in spring length, thus change in weight, before and after heat treatment. The sensitivity of the balance is 0.1 mg.

(2) Surface Area. Surface area measurements were performed using 200 mg samples of magnesium hydroxide slowly heated to the desired temperature under dynamic vacuum. CP-MgO was heated overnight for more complete dehydration. Final temperature was then maintained for 3 h and the weight of magnesium oxide was calculated from experimental weight loss. The Brunauer−Emmett−Teller (BET) one-point gas absorption method was employed using N_2 adsorption at liquid N_2 temperature to measure the surface area.[26]

(3) Surface Hydroxyl Groups. Using the sample and vacuum line from surface area analysis, measurement of surface hydroxyl groups was conducted.[27] With a static atmospheric pressure of dry nitrogen over the magnesium oxide sample, a 1 mL portion of 1.0 M solution of $Al(C_2H_5)_3$ in deoxygenated Decalin was slowly added. The mixture was allowed to react overnight producing a pressure, thus a volume, of ethane gas that was periodically measured during the reaction process. Note the reaction below:

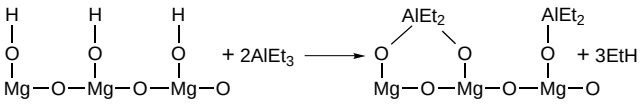

From the volume of ethane, the pressure (less solvent vapor pressure) and the temperature, the moles of ethane, thus the moles of hydroxyl groups, were calculated. Knowing the sample surface area allowed the final conversion to more useful units of hydroxyl groups per nm^2.

(4) Transmission Electron Microscopy. Transmission electron microscopy was used for AP-MgO and CP-MgO samples that were heat treated at 500 °C maintained overnight under dynamic vacuum of 1 mTorr, cooled to room temperature and sealed under Ar until studied.

(5) Atomic Force Microscopy (AFM). Imaging the sample surface was carried out using a commercial AFM instrument (SPM 30 from Wyco Co., Tucson AZ) in contact mode. A 100-μm-long cantilever with a spring constant of 0.0625 N/m and a Si_3N_4 tip was used. The force employed was about 78×10^{-9} N. The sample surfaces were scanned using the height mode, where the force, and hence the distance between the tip and the surface is kept constant. All images (256 × 256) pixels were recorded in air at room temperature using a slight filtering during the data acquisition. Different parts of the sample were investigated to make sure that the observed structure is representative and reproducible.

(6) Fourier Transform Infrared Spectrometry. Pellets 13 mm in diameter and ca. 30 mg were made of AP-$Mg(OH)_2$ and CP-$Mg(OH)_2$ using a Spectra-tech Inc. Model die 139 and a Carver model B laboratory press with ca. 7000 psi on the press. The pellets were transferred to the lower section of an in situ IR cell[28] and treated by ramping to 500 °C over 3 h and soaking at 500 °C for an additional 3 h. Room-temperature IR spectra were then recorded using a Perkin-Elmer 1330 infrared spectrometer with 256 scans, 2 cm^{-1} resolution, and aperture of 1.0 cm^{-1}.

(C) Adsorption of SO_2 on AP-MgO and CP-MgO. *(1) Pretreatment Temperature.* Loaded on the spring balance, 80 mg samples of AP-$Mg(OH)_2$ and CP-$Mg(OH)_2$ were slowly heated under dynamic vacuum to the desired temperature and maintained for 3 h. CP-MgO was heated overnight. The sample was then cooled to room temperature for 1 h and 20 Torr of SO_2 was introduced to the sample chamber, allowing static contact for 15 min, followed by 100 min of evacuation. The change in spring position, thus weight difference, was measured before and after heating and before and after evacuation. Evacuation removed the physically adsorbed SO_2 allowing the calculations of physically and chemically adsorbed amounts. To understand the effect of heat treatment temperature on adsorption abilities, this process was followed for preheating temperatures of 25, 120, 250, 300, 400, and 500 °C and, using the surface area determination, SO_2/nm^2 was calculated. The SO_2 used in these studies was 99.9+% pure purchased from Aldrich.

A duplicate study was completed for CO_2 on AP-MgO and CP-MgO heat treated at 500 °C only.

(2) Desorption of SO_2. Following the process described previously with 20 Torr of SO_2 statically in contact with AP-MgO, SO_2 was then steadily desorbed under dynamic vacuum at temperatures of 100, 200, 300, 400, and 500 °C at 0.5 h intervals and 500 °C overnight with spring balance positions, thus loading amount, calculated for each temperature.

(3) Pressure of SO_2. To understand the effect of pressure of SO_2 on adsorption, 100 mg samples of AP-$Mg(OH)_2$ and CP-$Mg(OH)_2$ were heated to 500 °C on the spring balance, maintaining the temperature overnight as discussed earlier, and exposed to incremental increases in pressure of SO_2 at room temperature. The pressures included are 10, 20, 40, 100, 200, 300, 400, and 741 Torr (atmospheric pressure). Static pressures of SO_2 were maintained until equilibrium loading was established.

(4) Oxygen Scrambling. To determine if SO_2 exchanges oxygen with the surface of the MgO, an isotopic scrambling study was conducted. Previous experiments showed that nanoscale MgO does exchange lattice oxygen and surface OH groups with water vapor.[16] A Perkin-Elmer QMass spectrometer 910 modified with an in situ reactor[17] was employed using the same column described earlier with an increased flow rate of 50 mL/min and temperatures of column and injector port at 120 °C. In short, 100 mg of AP-MgO, previously heated treated to 500 °C was transferred under inert atmosphere to the in situ reactor and attached in line with the GC/MS. To prepare $Mg^{18}O$, injections of 1 μL of $H_2{}^{18}O$ were initiated, and the effluent of each injection was studied. Injections of $H_2{}^{18}O$ ended when equilibrium conditions of the surface layer exchange were met; more then one layer of surface oxygens was exchanged at a reactor temperature of 500 °C. The reactor was then cooled to room temperature and 400 μL injections of SO_2 were initiated and the effluent studied by GC/MS.

(5) Powder X-ray Diffraction. A Scintag-XDS-2000 was used for powder X-ray diffraction spectra of AP-MgO heat treated at 500 °C for 3 h under dynamic vacuum and cooled to room temperature. The sample was then exposed to 20 Torr of SO_2 under static conditions, for 15 min and directly analyzed.

Results

(A) Characterization of AP-MgO and CP-MgO. *(1) Desorbed Gases during Heat Treatment.* Previous weight loss studies showed that AP-MgO lost more weight than CP-MgO during heat treatment (Figure 1); in fact, AP-MgO weight loss was higher than the expected stoichiometric value of 31% ($Mg(OH)_2 \rightarrow MgO + H_2O$). This was found, by IR studies, to be due to the loss of residual methoxy groups left on the surface after preparation.[19]

GC/MS analysis of the effluent produced during heat treatment of AP-MgO elucidated the differences found in IR spectra of heat treated AP-MgO and CP-MgO. AP-MgO spectra contained ν_{C-H} bands centered around 2800 cm^{-1} that corresponded to methoxy groups remaining on the surface until reaching 500 °C at which point they were removed. CP-MgO spectra did not

(25) Koper, O.; Li, Y. X.; Klabunde, K. J. *Chem Mater* **1993**, *5*, 500.
(26) Anderson, J. R. *Structure of Metallic Catalysts*; Academic Press: London, 1975.
(27) Sato, M.; Kanbayashi, T.; Kobayashi, N.; Shima, Y. *J. Catal* **1967**, *7*, 342.
(28) Matsuo, K.; Klabunde, K. J. *J. Org. Chem.* **1982**, *47*, 843.

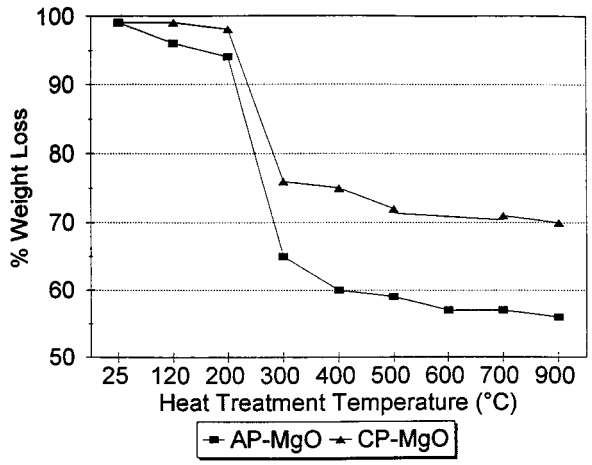

Figure 1. Percent weight loss verses heat treatment temperatures for AP-MgO and CP-MgO.

contain such peaks. Both spectra, however, did show ν_{O-H} peaks that persist even after 500 °C heat treatment. GC/MS results showed for AP-MgO that most of the water was removed at temperatures between 100 and 120 °C, yet there was continual dehydration through out the heating, with another resurgence peaking between 300 and 400 °C. The continual, yet varying, removal of water can also be monitored by IR and has been verified by various authors.[29] The first removal of water is expected since it is known that molecular water is removed at 100 °C, demonstrated by the lack of an adsorption band at 1600 cm^{-1}, leaving hydroxyls behind. The bond strengths of these hydroxyls vary due to their bonding site, coordination to the surface, crystal face, and chemical environment. The actual nature of the bonds, however, is a point of controversy.[20] In general, the sharp adsorption band near 3750 cm^{-1} is assigned to ν_{OH} of isolated surface OH groups and the broad band at 3650−3200 cm^{-1} to hydrogen-bonded surface OH groups.[29] The second, less extensive, removal of water between 300 and 400 °C removed water molecules hydrogen bonded via surface hydroxyls.[30] Carbon dioxide was eliminated mostly from 100 to 200 °C and increased again from 400 to 500 °C. This final removal of CO_2 corresponded to the final removal of methoxy groups at 500 °C. The pattern of CO_2 removal suggested that there were at least two forms of carbon species on the surface having different bond strengths. IR studies suggested that the more tightly bound methoxy groups were removed in the latter heat treatment. Due to the nature of these experiments, quantitative evaluation of CO was not possible, but previous work has shown that it is a product, along with H_2.[19] The unbalanced reaction below shows the products formed:

$$Mg(OH)_2(OCH_3)_x \rightarrow MgO + H_2O + CO + H_2 + CO_2$$

(2) Surface Area. Surface area determinations for AP-MgO and CP-MgO at heat treatment temperatures of 25, 120, 250, 300, 400, and 500 °C were completed using the BET one-point method. AP-MgO consistently had higher surface areas (350−450 m^2/g) than CP-MgO (50−250 m^2/g) with maximum surface area for both samples attained near 300 °C heat treatment temperatures.[19] It is believed that above 400 °C, sintering, or structural rearrangement, is initiated, transforming less-stable high-index planes into domains of more stable (100) planes,[20] thus leading to lower surface areas and more crystalline material. Also, this high-temperature annealing process can remove surface defects while forming a more perfect crystal structure.

(3) Surface Hydroxyl Groups. Surface hydroxyl groups remaining on the surface after heat treatments of 120, 300, 400, 500, and 700 °C were measured as reported earlier.[19] With increase in heat treatment temperature for both samples, comes an anticipated decrease in OH groups (from 8/nm^2 to about 1/nm^2; note that maximum coverage would be 12/nm^2). Agreeing with the IR studies, even at temperatures of 700 °C, isolated OH groups remain on AP-MgO and CP-MgO, with AP-MgO spectral peaks having stronger intensity. Also note that the OH/nm^2 is lower for AP-MgO than for CP-MgO until temperatures above 500 °C were reached, probably due to the presence of residual methoxy groups, instead of OH groups, still on the surface of AP-MgO until 500 °C.

(4) Transmission Electron Microscopy. TEM prints of AP-MgO and CP-MgO clearly show a major difference in morphology.[19] AP-MgO appears as collections of weakly attracted polyhedral particles of 2−6 nm in diameter, while CP-MgO appears as, on average, 9 nm thick hexagonal plates. Previous XRD studies of AP-MgO and CP-MgO confirm these average crystallite sizes, determined from peak broadening using the Scherrer equation.[22,23] Also, the crystal structure of both samples was determined to be periclase MgO. Figure 2a shows a high-resolution TEM micrograph of an aggregate of AP-MgO crystallites. On the fringe particles lattice spacings are discernible and appear to be ordered over a 4−6 nm range. Figure 2b is an AFM print of a pressed powder, showing the morphology of larger aggregates of nanoparticles. In keeping with the accepted cubic structure of MgO, idealized models of these two types of MgO are shown (Figure 3). Assuming cubic morphology with defects, such as its corners removed, for small particles like AP-MgO, the cuboctahedron model was drawn. It should also be noted that the AP-MgO model surface has more higher index planes than CP-MgO, which mainly shows more thermodynamically stable (100) faces. The AP-MgO model also has more edge and corner sites. In these models, AP-MgO has square faces as (100) surfaces, and hexagonal faces as (111)surfaces, whereas CP-MgO has (100) surfaces on the hexagonal faces and two of the parallel rectangular faces and (110) surfaces on the other four rectangular faces. The (110) surfaces are made of steps, therefore, having many 4-coordinate ions on the face, while the (111) surface is formed from missing corners, thus having many 3-coordinate ions.

(5) Fourier Transform Infrared Spectrometry. Spectra of AP-MgO and CP-MgO after 500 °C heat treatment showed a peak centered at ca. 3750 cm^{-1}; yet for AP-

(29) (a) Coluccia, S.; Lavagino, S.; Marchese, L. *Mater. Chem. Phys.* **1988**, *18*, 445. (b) Tsyganko, A. A.; Filmonov, V. N. *J. Mol. Struct.* **1973**, *19*, 579. (c) Shido, T.; Asakura, K.; Iwasawa, Y. *J. Chem. Soc., Faraday Trans 1* **1989**, 85, 441. (d) Boehm, H. P.; Knözinger, J. In *Catalysis-Science and Technology*; Anderson, J. R., Boudart, M., Eds.; Springer: Berlin, 1983; Vol. 4, p 39. (e) Davydov, A. A. In *Infrared Spectroscopy of Adsorbed Species on the Surface of Transition Metal Oxides*; Rochester, C. H., Ed.; Wiley: Chichester, 1990. (f) Little, L. H. *Infrared Spectra of Adsorbed Species*; Academic Press: New York, 1966.

(30) Dùnski, H.; Józwiak, W. K.; Sugier, H. *J. Catal.* **1994**, *146*, 166.

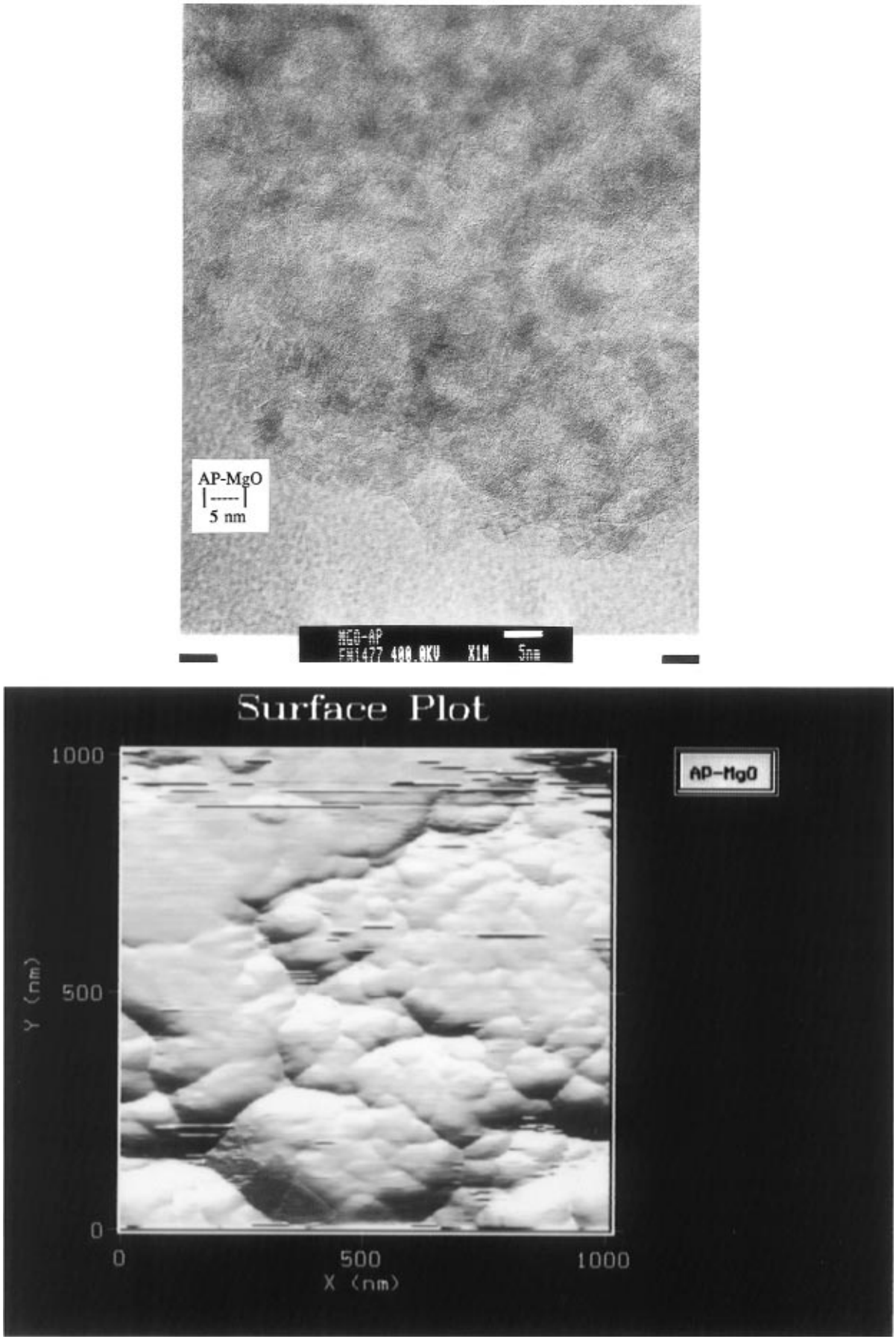

Figure 2. (a, top) TEM print of AP-MgO, which shows an aggregate of nanocrystals. Note the lattice planes that are ordered for about 4−6 nm (bar is 5 nm). (b, bottom) Atomic force micrograph (AFM) of a pressed pellet of AP-MgO, showing aggregates.

MgO this peak was noticeably more intense and sharper. It is known that particle size affects spectra, with larger particles, here CP-MgO, giving lower intensity and resolution. As mentioned earlier, this peak was as-

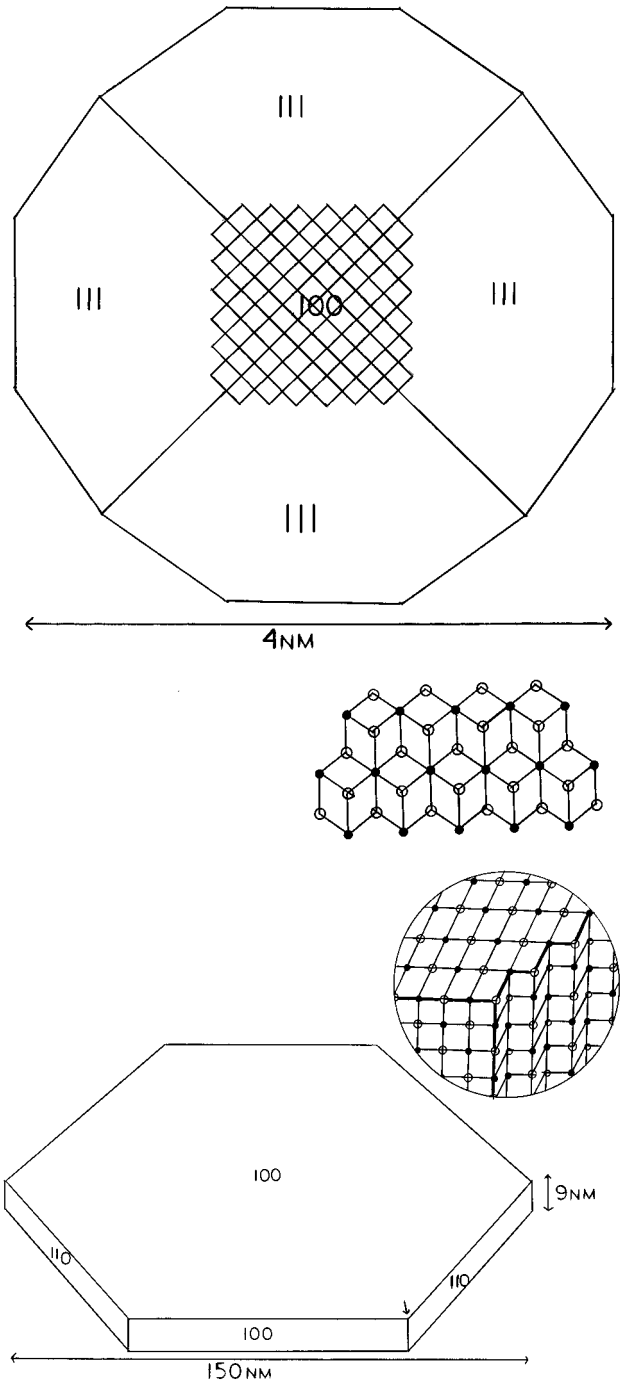

Figure 3. Idealized illustrations to scale of average crystallites of nanoscale AP-MgO and microscale CP-MgO. (a) AP-MgO average crystallite with an insert showing a (111) crystal face. (b) CP-MgO average crystal with an insert showing one corner in detail.

signed to isolated OH groups. Employing high-temperature degassing above 700 °C, Knözinger and co-workers found that this band separates with the higher frequency component attributed to 1-coordinated OH groups (type A) and the lower frequency component to higher coordination OH groups (type B).[20] The pK_a of the surface hydroxyl at 3752 cm^{-1} was reported to be 15.5 ± 0.4.[31]

The region below 2000 cm^{-1} is harder to assign and is therefore rarely discussed in the literature. In general, these peaks are related to surface species such as hydrides, OH bending modes, carbonates, and bicarbonates, with some peaks yet to be identified.

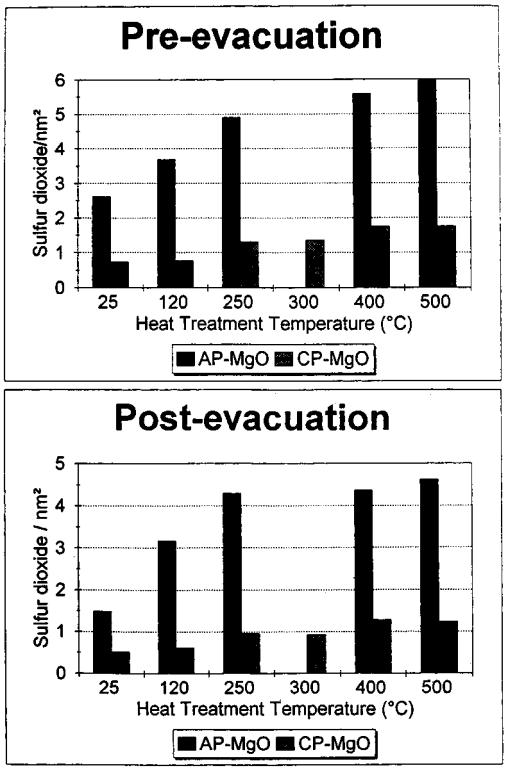

Figure 4. Number of SO_2/nm^2 adsorbed on AP-MgO and CP-MgO heat treated at various temperatures: Pressure of SO_2 = 20 Torr. Taller bars are for AP-, and shorter bars for CP-.

(B) Adsorption of SO_2 on AP-MgO and CP-MgO. *(1) Pretreatment Temperature.* The amount of SO_2 adsorbed on AP-MgO and CP-MgO was measured as SO_2/nm^2 at various heat treatment temperatures of 25, 120, 250, 300, 400, and 500 °C. The results are shown in Figures 4 and 5. The preevacuation amounts include physically and chemically adsorbed SO_2 species. Since these calculated results are already corrected for surface area, they are in units of SO_2/nm^2, it is clearly shown that more SO_2 is adsorbed on AP-MgO than on CP-MgO per surface unit. Thus, it unmistakably implies that AP-MgO must have intrinsically different surface characteristics and perhaps different or more numerous active sites, allowing higher reactivity with SO_2. Comparing preevacuation results with postevacuation results, is clear that most of the adsorption is chemisorption. For both samples, the adsorbing ability increases with preheat treatment temperature. Noting that the samples began as $Mg(OH)_2$ and were dehydrated with heat treatment, an explanation for this is as follows. Dehydration opened sites for adsorption formerly occupied by water, hydroxyls, and hydrogen atoms. For AP-MgO additional sites formerly occupied by methoxy groups and other carbon species were also formed at 500 °C. A comparison gas, CO_2 was also adsorbed an AP-MgO and CP-MgO heat treated at 500 °C (Figure 5). Once again, preevacuated and postevacuated results, showing total adsorbed species and chemisorbed species, respectively, demonstrated that most of the CO_2 was chemisorbed on both MgO samples. Surface area corrected results show that significantly more CO_2 was adsorbed on AP-MgO than on CP-MgO. It can also be noted that SO_2 being a stronger acid gas, adsorbed three

(31) Hair, M. L.; Hertl, W. *J. Phys Chem.* **1970**, *74*, 91.

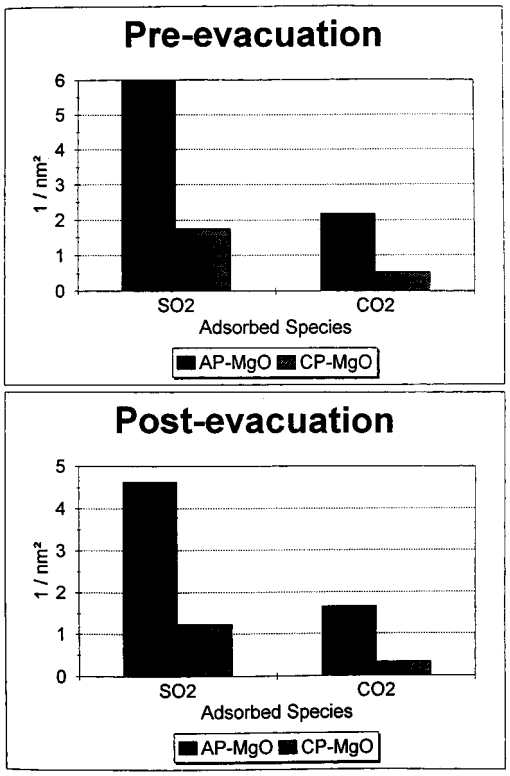

Figure 5. Number of SO_2/nm^2 and CO_2/nm^2 adsorbed on AP-MgO and CP-MgO preheat treated at 500 °C: Pressure = 20 Torr. Taller bars are for AP-, and shorter bars for CP-.

times more than CO_2. Therefore, it appears that CO_2 is more selective than SO_2 (which probes all basic sites whatever their strength).

(2) Desorption of SO_2. AP-MgO heat treated at 500 °C and exposed to SO_2 was systematically heated under dynamic vacuum on the spring balance to observe the desorption of SO_2. The desorption of SO_2 did not appreciably occur until temperatures of 300 °C and greater were met. By 500 °C, 0.90 SO_2/nm^2 remained on the surface and 0.63 SO_2/nm^2 after overnight treatment.

(3) Pressure of SO_2. Samples of AP-MgO were heat treated at 500 °C, cooled to room temperature and exposed to increasing pressures of SO_2. Once again, the results were calculated in SO_2/nm^2 to correct for surface area differences. Unexpectedly, CP-MgO adsorbed more SO_2 than AP-MgO at pressures above 50 Torr. Both isotherms showed continual increases which begin to level off above 200 Torr. This data gave a "normal" isotherm for chemisorption. Assuming the high-pressure range is relatively linear, an extrapolation to the uptake axis gave uptakes of 7.0 and 11 SO_2/nm^2 for AP-MgO and CP-MgO, respectively. Note that, while at a pressure of 20 Torr, AP-MgO adsorbed more SO_2 per unit surface area than CP-MgO, but at higher pressures the reverse is true. This prompted further investigation. A similar study measuring adsorption of SO_2 over time showed that, for pressures of 100, 40, 20, and 10 Torr, 80% of the SO_2 was adsorbed in the first 10 min and leveled off quickly thereafter. For pressures of 400 and 740 Torr, the saturation values were still not reached in the 4 h experiment.

(4) Oxygen Scrambling. After exchange of AP-MgO with $H_2{}^{18}O$ at 500 °C,[16] a sample of AP-$Mg^{18}O$ was treated with 400 μL gaseous SO_2 injections. The first few injections caused the desorption of mixed CO, $C^{18}O$, CO_2, $CO^{18}O$, and $C^{18}O^{18}O$ plus a mixture of H_2O and $H_2{}^{18}O$. Only after the twelth injection, a mixture of SO_2, $SO^{18}O$, and $S^{18}O^{18}O$ was evolved while the sample was maintained at 500 °C; the major component was the single labeled component $SO^{18}O$.

These experiments point out that at 500 °C, SO_2 and CO_2 (as carbonate) are exchanging oxygens with surface and lattice ^{18}O. Furthermore, SO_2 displaces surface carbonate.

Powder X-ray diffraction of the SO_2 treated $Mg^{18}O$ showed only the MgO periclase structure, verifying that the bulk structure was not changed.

Discussion

(A) Morphological Differences. Normally, crystallites of MgO have cubic rock salt morphology,[10,23,24] while $Mg(OH)_2$ crystallites exhibit hexagonal plate morphology. Electron micrographs confirm the mostly cubic shape of normal MgO crystals showing predominately stable (100) planes.[32,33]

It has also been shown that the choice of precursor and the manner of preparation of MgO produces different morphologies and properties.[10,20,23,24] Herein both CP-MgO an AP-MgO were produced by the dehydration of $Mg(OH)_2$. In the case of CP-MgO, remnants of the hexagonal structure of $Mg(OH)_2$ are partly preserved. However, in the case of AP-MgO, the precursor is a gel like disoriented $Mg(OH)_2$ and dehydration leads to very small polyhedral particles with an abundance of defects, steps, and truncated corners, resulting in the exposure of various crystal planes (see Figures 2 and 3). Therefore, AP-MgO possesses a large surface moieties/bulk ratio and more ions in 4-coordinate and 3-coordinate sites than CP-MgO. It seems inevitable that AP-MgO should also expose more higher index planes, such as (111), than CP-MgO. Furthermore, AP-MgO exhibits a pore structure due to the loose packing of the small, polyhedral 4 nm crystallites.[19]

Do these morphological differences and crystallite size differences cause the MgO surfaces to have different chemistry? One indication that the answer is "yes" was found in careful studies of residual surface-OH groups, where the frequency of geminal OH was lower on AP-MgO, and Bronsted acidity was also lower, suggestive of placement of the −OH groups on lower coordination sites.[19] Of course, removal of surface −OH groups is dependent on temperature opening up Lewis base sites, O^{2-}, which reach a maximum at 500−600 °C.[34,35]

(B) Chemisorption of SO_2 and CO_2 at Low Pressures (20 Torr). Perhaps the most important difference in chemistry is demonstrated by the fact that at low pressures, much more SO_2 is adsorbed by AP-MgO per nm^2 then on CP-MgO. This held true at all preheat treatment temperatures. Similar results were found with CO_2, although CO_2 was adsorbed in smaller amounts overall (see Figures 4 and 5).

If this greater capacity /nm^2 to adsorb SO_2 and CO_2 is due to a greater surface reactivity (such as greater

(32) Goodsel, A. J.; Low, M. J. D.; Takezawa, N. *Environ. Sci. Technol.* **1972**, *6*, 268.
(33) Anderson, J.; Harlock, R. F.; Oliver, J. F. *Trans. Faraday Soc.* **1965**, *61*, 2754.
(34) Evans, J. V.; Wateley, T. L. *Trans. Faraday Soc.* **1967**, *63*, 2769.
(35) Busca, G.; Lamotte, J.; Lavalley, J. C.; Lorenzelli, V. *J. Am. Chem. Soc.* **1987**, *190*, 5197.

Table 1. IR Bands for Carbonates on MgO

				Bicarbonate[a]				
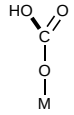	1655			1650	1638	1658	AP-MgO	CP-MgO
	1405			1417−1448	1420/1459	1419	1480	
	1220			1220−1229	1210	1223	1250	
	1040							
	840							
				Monodentate Carbonate[b]				
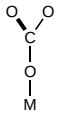	1510		1550	1538−1580	1572/1518	1526	1590	1510
	1390		1410	1420	1420/1385	1421	1510	1410
	1035		1050			1075	1415	small
	865		860				865	
				Bidentate Carbonate[c]				
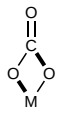	1665	1670/1650	1670/1630	1700				1385
	1325	1320/1280	1330/1280	1357−1380				1335
	1005		1030/950					850
	850		855/830					
ref	34	35	36	37	38	39	this work	this work

[a−c] Band assignments for the first three bands of each carbonate. (*a*) Asymmetric stretching, symmetric stretching, and COH bending. (*b*) Asymmetric stretching, symmetric stretching, and symmetric stretching. (*c*) Symmetric stretching, asymmetric stretching, and symmetric stretching.

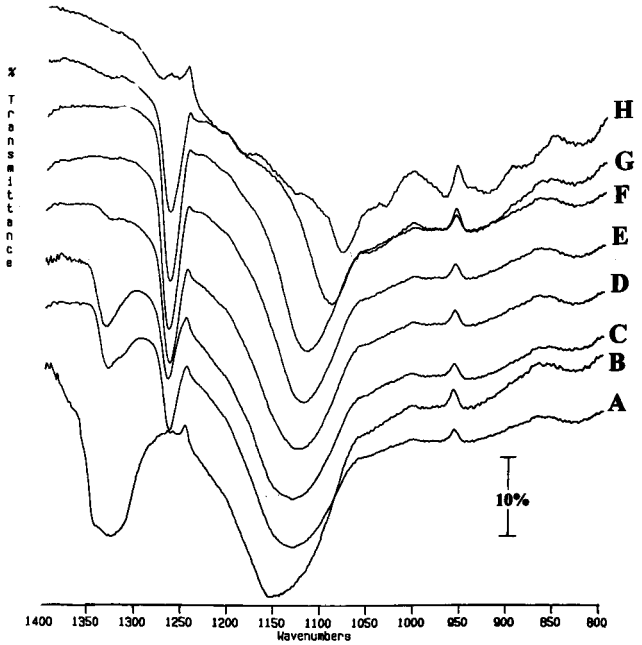

Figure 6. Subtracted regions of IR spectra of SO_2 adsorbed on AP-MgO: (a) after SO_2 adsorption at 100 Torr; (b) after 4 h sample evacuation at 25 °C; (c) after 18 h evacuation; (d) after 42 h evacuation; (e) evacuation at 100 °C; (f) 150 °C; (g) 300 °C; (h) 500 °C.

O^{2-} basicity), then IR studies of the adsorbed SO_2 or CO_2 might be informative.

Adsorption of CO_2 produces a set of surface carbonates, and the wavenumber difference between the asymmetric and symmetric stretching bands appears as a function of the partial charge on the surface oxygen site. Bicarbonates, monodentate carbonates, and bidendate carbonates have all been observed by several groups, as summarized in Table 1.

Our results for AP-MgO and CP-MgO are also tabulated in Table 1. Judging from the peaks present and their intensities, it is clear the AP-MgO has much more monodentate carbonate present, while CP-MgO has more bidentate carbonate. In addition, only AP-MgO exhibited a small amount of bicarbonate species. These results are consistent with earlier findings concerning surface −OH groups; that is, CP-MgO exhibited more geminal and/or adjacent −OH species, whereas AP-MgO more isolated/monodentate. The evidence points out that the very small size and, the predominance of edge/corner sites encourages the formation of monodentate type species on AP-MgO.

Table 2. IR Bands for SO_2 Species on MgO

SO_2 species	IR bands (cm^{-1})	AP-MgO	CP-MgO
SO_2 gas	1360		
	1154		
SO_2 physisorbed	1336		
	1149		
SO_2 monodentate	1323	1330	1320
chemisorbed	1140	1135	1140
bidentate sulfito	1134		
	1122	1120[a]	1120[c]
	1062		
	954		
monodentate sulfito	1088	1090[b]	1090[b]
	1041		
	956		
ref	32	this work	this work

[a] Appears upon extended evacuation. [b] Appears upon heating. [c] Appears upon evacuation, but more quickly than with AP-MgO.

Looking at SO_2 adsorbed species, Figure 6 shows FTIR (subtracted) spectra of SO_2 adsorbed at room temperature on a 500 °C preheat treated sample of AP-MgO. Initial adsorption, after 18 h of evacuation, 42 h of evacuation, and evacuation at 152 and 500 °C the region of 1300−1350 and 1050−1200 cm^{-1} are shown, covering the two main bands of SO_2.

Table 2 shows the assigned bands for SO_2 adsorbed on MgO by Goodsel and co-workers.[32] Essentially all of these species were also observed in our study. Two predominant bands near 1330 and 1150 are due to gaseous as well as physisorbed SO_2. They shift somewhat upon chemisorption.

(36) Fukunda, Y.; Tanabe, K. *Chem. Soc. Jpn.* **1973**, *46*, 1616.
(37) Lercher, J. A.; Colombier, C.; Noller, H. *J. Chem. Soc., Faraday Trans. 1* **1984**, *80*, 949.
(38) Rethwisch, D. G.; Dumesic, J. A. *Langmuir* **1986**, *2*, 73.
(39) (a) Philipp, R.; Omata, K.; Aok, A.; Fujimoto, K. *J. Catal.* **1992**, *134*, 422. (b) Philipp, R.; Fujimoto, K. *J. Phys. Chem.* **1992**, *96*, 9035.

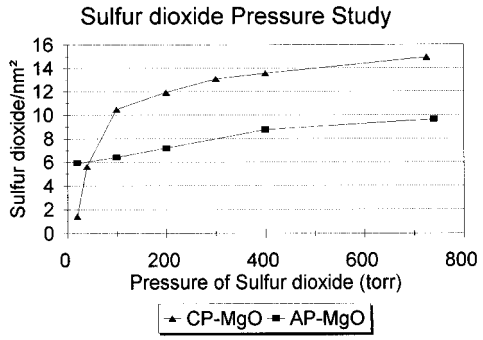

Figure 7. Amount of SO_2 adsorbed on AP-MgO and CP-MgO with increasing pressures. After evacuation these adsorption values fall to about 5 SO_2/nm^2 for AP-MgO and also about 5 SO_2/nm^2 for CP-MgO.

On AP-MgO the 1330 cm^{-1} band disappears after the 42 h evacuation at room temperature and the 1150 cm^{-1} band progressively shifts to about 1120 cm^{-1}. Upon heating and evacuation this band further shifted to about 1090 cm^{-1}, which indicates that on AP-MgO the SO_2 monodentate chemisorbed is lost upon extended evacuation. However, bidentate sulfito is formed, but upon further heating appears to be converted to monodentate sulfite.

These results are in agreement with Goodsel and coworkers.[32]

However, in the case of CP-MgO, more complex spectra were observed, and the SO_2 monodendate chemisorbed species appeared at 1320 cm^{-1} and this band disappeared after 18 h evacuation (instead of 42 on AP-MgO). A similar progression to bidenate sulfite and then monodentate sulfite was observed.

Accordingly, SO_2 is a Lewis acid initially probing Lewis base sites, O^{2-}, then upon heating rearranging to form sulfite as shown below (going from chemisorbed SO_2 to bidentate sulfito to monodentate sulfite):

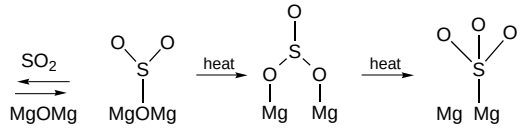

The spectra were very similar on AP-MgO and CP-MgO, the only difference noted was that the AP-MgO retained the SO_2 monodentate chemisorbed for a longer time, and the adsorption at 1330 was slightly higher in energy (1330 verses 1320 cm^{-1}) than on CP-MgO. Thus, the only conclusion is that the chemisorbed SO_2 was more tightly held on AP-MgO.

(C) Pressure Effects on Adsorption. In Figure 7 are shown the results of adsorption of SO_2 at various pressures. Note that at 20 Torr about 6/nm^2 are adsorbed on AP-MgO verses 2/nm^2 on CP-MgO. However, as the pressure is raised to 100, 200, and 700 Torr the amount adsorbed increases to around 10/nm^2 for AP-MgO but goes all the way up to 15/nm^2 for CP-MgO.

Using a cross-sectional area of 19.2 $Å^2$ for the SO_2 molecules,[33] it can be calculated that 5.2 SO_2 molecules/nm^2 MgO would form a monolayer. Indeed, this is very close to the amount that actually is adsorbed at 20 Torr on AP-MgO. So as the pressure is raised to 100 Torr or higher, multilayers of SO_2 are adsorbed. It was noted, however, that upon evacuation the amounts adsorbed for both AP- and CP-MgO fell to about 5 SO_2/nm^2, suggesting that the multilayers (second and third) on CP-MgO are physisorbed, not chemisorbed. So the question to answer is, Why should CP-MgO be more capable of this multilayer physisorption?

The IR studies are not of much help here, since SO_2 adsorbed on both AP-MgO and CP-MgO yield quite similar spectra, yet we do know that the morphologies of the two samples are very different. Perhaps a reasonable rationale is that CP-MgO, with its more ordered microcrystals with large exposed areas of the (100) crystal face is able to physisorb SO_2 in a more ordered fashion, thus more multilayer SO_2 can "fit" down on the surface. This may represent an example when self-organization of multilayers allows more close neighbors, a more "crystalline" denser array of adsorbate molecules.

Conclusions

In comparing nanoscale AP-MgO with microscale CP-MgO particles, several significant differences were encountered. First of all, the particle morphology is very different, AP-MgO particles are made up of 4 nm polyhedrals with a cubic internal structure but with an abundance of edge and corner sites and crystal planes, whereas CP-MgO exists as 150 nm in length hexagonal plates with larger surfaces of (100) crystal planes and relativity fewer edge and corner sites and fewer (111) and (110) exposed planes.

Adsorption of CO_2 and SO_2 at low pressures (20 Torr) leads to more molecules adsorbed/nm^2 on AP-MgO than CP-MgO and a monolayer of 6 SO_2/nm^2 MgO was formed on AP-MgO. However, at higher pressure, multilayers are weakly adsorbed and in this instance CP-MgO is the superior adsorbent apparently due to the formation of more ordered, denser multilayers. Overlays of IR spectra of adsorbed CO_2 and SO_2 suggest that monodentate species are favored on AP-MgO whereas bidentate structures are favored on CP-MgO, apparently due to the different morphologies of the crystallite. In the case of SO_2, the monodentate chemisorbed was held more strongly on the nanoscale AP-MgO.

These results further reinforce the idea that nanoscale particles do exhibit unique surface chemistry.

Acknowledgment. The support of the Army Research Office is acknowledged with gratitude. We thank S. Rice of McCrone Associates for skillful TEM investigations.

CM950583P